Research Statement

John B. Greer

Many current scientific and mathematical problems require a careful combination of analysis and computation. Modern computing power allows the simulation of complicated nonlinear PDEs modeling physical phenomena, often when little has been proved rigorously about the equations themselves. This clearly benefits modern research, but care must be taken to ensure the accurate use of numerics and the mathematical viability of PDE models. Today's scientist must often understand both the mathematics of the nonlinear phenomena they study and the practical details of computation.

My research interests lie on this boundary between rigorous mathematical analysis and the design of numerical methods. Highlights of my past achievements include:

1. **Analysis of fourth-order PDEs used for image denoising, including some of the first rigorous results for equations of their type.**

2. **Numerical analysis that lead to significant improvements of a new method for computing PDEs on surfaces.**

3. **Analysis of coarsening in discrete evolution equations from image processing, population dynamics, and granular flow.**

Although these topics touch a wide range of mathematical applications, each requires an understanding of nonlinear PDEs and the ability to design and implement practical numerical methods. I discuss each of these achievements in sections 1-3 then move on to discuss current projects and future goals in Section 4.

1 Nonlinear diffusions for image processing.

Work in fields as far-reaching as medicine, astronomy, and national security requires the retrieval of data from images. These images often include high frequency noise that must be removed before any data analysis. Recently mathematicians and engineers have turned to nonlinear PDEs for this denoising process, using PDEs for insight in the development of numerical algorithms that may be directly used on digital images. In some cases the PDEs are actually ill-posed with little known about their solutions, but even lacking a complete theory for the equations, discretizations (the primary interest for applications to digital images) are typically well defined.

This section focuses on my doctoral work, which concerned the analysis of new nonlinear fourth-order PDEs recommended by engineers for image denoising. These PDEs have structures similar to an ill-posed second-order PDE, for which discretizations have been successfully used for image denoising. The work discussed in this section mainly focuses on the analysis of the fourth-order PDEs in the continuum, but I return to their ill-posed second-order analogue in Section 3, where I discuss my recent analysis of a related class of ill-posed nonlinear diffusions.

1.1 Second-order PDEs for image denoising

Twenty years ago, images were denoised by linear filtering, which is equivalent to using the noisy image as an initial condition for the heat equation. Although successful at removing noise, linear filtering also blurred edges, so researchers turned to nonlinear diffusions like

$$u_t = \nabla \cdot \left(g\left(|\nabla u|\right) \nabla u \right), \tag{1}$$

where the function $g(s)$ is small for large s, thus minimizing diffusion near the edges of images [21, 22]. The function u represents the intensity of the processed image, with u at time $t = 0$ being the initial unprocessed image. Time serves as an artificial variable corresponding to the amount of processing done. The two most successful examples of (1) are the *Perona-Malik Equation*, which typically has

$$g(s) = \frac{1}{1 + \left(\frac{s}{k}\right)^2} \tag{2}$$

with $1/k$ scaling like the pixel size, and *Total Variational (TV) flow*, where $g(s) = 1/s$.

1.2 My contribution: Rigorous analysis of fourth-order nonlinear diffusions

Although effective at denoising, discretizations of (1) typically produce piecewise constant images, giving "blocky" results. Attempts to preserve continuous color gradients led to experiments with fourth-order diffusions like

$$u_t + \nabla \cdot (g(\Delta u) \nabla \Delta u) = 0, \tag{3}$$

introduced in [24], and the higher-order analogue of TV flow introduced in [19]:

$$u_t + \Delta \nabla \cdot \left(\frac{\nabla u}{|\nabla u|} \right) = \lambda (f - u). \tag{4}$$

Prof. A. Bertozzi (UCLA Mathematics) and I proved the first analytical results for some of these new fourth-order diffusions. In [14], we used energy methods to prove well-posedness of a class of H^1 diffusions for image processing. In [7], we proved that (3), with g given by (2) has smooth solutions locally in time in $\mathbb{R}^2$, and globally in time in $\mathbb{R}$. Since fourth-order PDEs have no maximum principle, our analysis relies on an *entropy* of (3). This *entropy* is an integral of the solution u with bounded growth. We show that the integral's controlled growth implies that solutions must maintain a certain amount of regularity. This technique has also been used to prove regularity results for solutions of PDEs related to the dynamics of thin films [4, 6], and in [7] we examine a link between (3) and thin film equations. Our regularity results for (3) were surprising, since the equation bears much resemblance to the ill-posed Perona-Malik equation. **(Published in [7, 14, 15])**

Prof. Bertozzi and I worked with Prof. S. Osher (UCLA Mathematics) and Dr. K. Vixie (Los Alamos National Lab) to analyze (4). Computing (4) or its second-order counterpart requires regularizing the step function $H(\nabla u) = \frac{\nabla u}{|\nabla u|}$ to avoid division by zero. **We proved rigorous results for a class of regularizations of the second and fourth-order TV equations.** In particular, we showed that regularizations of (4) must be chosen carefully, whereas most standard regularizations are adequate for second-order TV. **(Published in [8])**

2 PDEs on surfaces

Phenomena in scientific areas including biology, fluid dynamics, and electromagnetism may be modeled by PDEs on surfaces. A portion of my postdoctoral work concerned the analysis and implementation of a recently designed method for solving PDEs on implicit surfaces. I describe this new method in Section 2.1 then discuss my own contributions in sections 2.2 and 2.3.

2.1 Solving PDEs on surfaces.

Until recently, computing PDEs on surfaces required surface parametrization or triangulation, both of which have drawbacks; for example, parametrizations usually require patching to connect different parametrization neighborhoods, and triangulated surfaces lack well-defined geometric properties. Furthermore, convergence of numerical schemes on triangulated surfaces remains less understood than convergence on Cartesian grids. To avoid these difficulties, Bertalmio et al. [5] introduced a method for solving PDEs on general smooth geometries

Figure 1: A moment in the evolution of the Cahn-Hilliard equation on the Stanford Bunny. The bunny is represented by a level set of a function in the embedding space. Computations required only finite differences on a Cartesian grid.

using only finite differences on a Cartesian mesh. By representing the surface S as the zero level set of a function ϕ defined in $\mathbb{R}^N$, geometric properties such as the surface normal and mean curvature may be determined by calculating derivatives of ϕ in the embedding space. Furthermore, computing the PDE in Eulerian coordinates only requires standard finite difference schemes in the embedding space [5, 1, 26].

2.2 My contribution: Fourth-order PDEs on surfaces

I worked with Professors A. Bertozzi (UCLA Mathematics) and G. Sapiro (UMN Electrical and Computer Engineering) to improve upon the methods of [5] to solve fourth-order PDEs on smooth surfaces of arbitrary geometry. The higher order equations introduce many challenges that are of little consequence for first and second-order PDEs; for example, stability restrictions for time stepping fourth-order equations require using implicit schemes, unlike most previous work on solving PDEs on implicit surfaces. We derived semi-implicit schemes using convexity splitting ideas explored in [11, 12] and presented a new means of combining convexity splitting schemes with ADI methods. We applied our methods to linear fourth-order diffusion, the Cahn-Hilliard equation (see Figure 1), and a recently derived model for surface tension driven flows on curved substrates. **(Published in [16])**

2.3 My contribution: An improved Eulerian formulation

Despite its elegance, the method introduced in [5] has a few drawbacks. Since the Eulerian representation of the surface PDE is defined on a larger domain in one higher dimension, one typically reduces computation by working in a small band around the surface. Boundary conditions required for computation can adversely affect numerical solutions, even though they have no effect on analytic solutions of the Eulerian representation. Any initial data must be extended off of the surface to the larger domain, and one typically requires the initial condition to be constant normal to the surface to reduce discretization errors by minimizing variations in the solution off of the zero level set. Unfortunately, the solution of the Eulerian PDE does not retain this property at later times, and as a result, long-time calculations of the PDEs often require intermittent re-extension of the data off of the surface to offset the effects of both boundary conditions and discretizations that include points from different level sets of ϕ [16, 26]. Finally, diffusion equations pose some trouble, as their Eulerian representations are degenerate diffusions in the embedding space (diffusion only occurs tangent to the surface).

I introduced an improvement of the method that is no more difficult to implement, requires no re-extension of the surface data, has simple boundary conditions associated with its Eulerian representation,

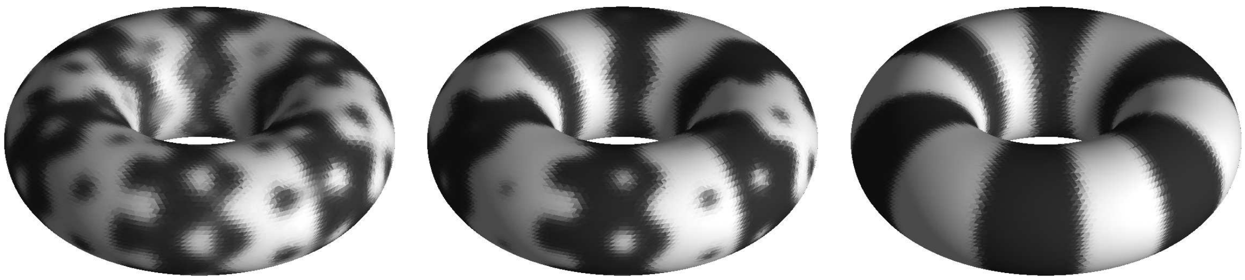

Figure 2: The Allen-Cahn equation on the curved torus, computed using only finite differences on a Cartesian mesh. The interface between the black and white regions undergoes motion by mean curvature.

and results in non-degenerate diffusion equations. I accomplished this by solving a different PDE in the neighborhood of S: at points on the surface, this new PDE is identical to that of the original method, but it differs at points off the surface, where it takes curvatures of the different level sets of ϕ into account. The modification's advantages result from a distinguishing property of this new PDE: given initial data that is constant in the direction perpendicular to the surface, the solution retains this property for all later times. **(To appear in J. Sci. Comp. – currently published on-line: [13])**

3 Ill-posed nonlinear diffusion equations.

Section 1.1 introduced the Perona-Malik method for image denoising, where the noisy image serves as the initial condition for a centered discretization of (1) with g given by (2). Although this PDE is ill-posed for fixed k in (2), k is actually chosen to scale like $1/h$ in applications to image processing (h denotes the grid/pixel size), and in fact (1) is not the $h \to 0$ limit of this discretization when k depends on h. Although (1) has been used for insight in the behavior of Perona and Malik's method, the PDE is often misleading, and accurate analysis of their method must focus on the *discretization*.

Similar relationships between discretizations and ill-posed diffusion equations arise in areas outside of image processing; examples include a model of shear bands in a granular medium [25] and a model for population aggregation under local reinforcement [20]. Part of my postdoctoral work concerned analysis of discretizations connected to these areas. I introduce the discretizations in Section 3.1 and describe my analysis in Section 3.2.

3.1 Discretizations of ill-posed diffusions.

The standard discretization of (1) in one dimension is strongly related to the system

$$\frac{d}{dt}v_i = \frac{R(v_{i+1}(t)) - 2R(v_i(t)) + R(v_{i-1}(t))}{h^2} \quad i = 0,\ldots,N-1 \quad h = \frac{1}{N} \tag{5}$$

which is a gradient descent of the energy

$$E(v) = \frac{1}{N}\sum_{i=1}^{N-1} f(v_i) \quad \text{with} \quad f(s) = \int_0^s R(\xi)d\xi$$

in the discrete H^{-1} norm. For convex f, Equation (5) is a convergent (as $h \to 0$) approximation of the parabolic equation

$$v_t = (R(v))_{xx}. \tag{6}$$

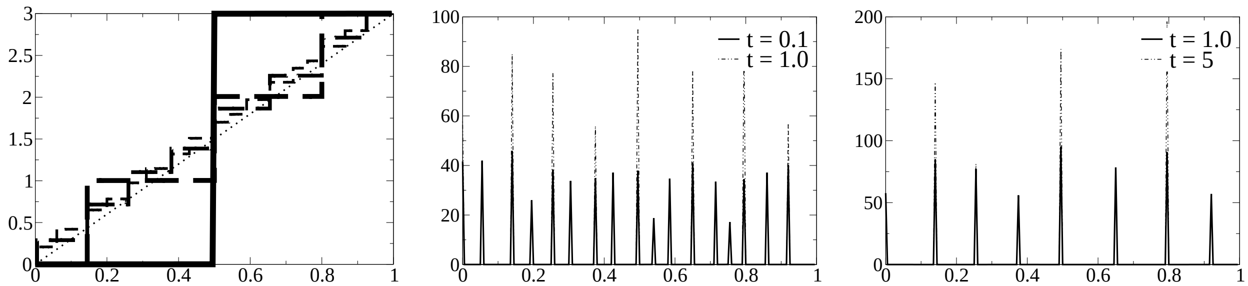

Figure 3: The left figure shows *staircasing* in a discretization of the one-dimensional Perona-Malik equation (7) with $g(s)$ given by (2). Thicker lines denote later stages of evolution. The initial condition is a small perturbation around a straight line with slope $m = 3$. The solution's discrete derivative satisfies (5), which typically behaves as shown in the middle and right figures.

However, equations like (1) with the nonlinearity (2) arise from a special class of *non-convex* functions $f(s)$ that are convex for small s and concave for large s. Letting $R(s) = g(s)s$ and $v = u_x$, a direct link may be established between (6) and the one-dimensional restriction of (1)

$$u_t = [g(u_x)\, u_x]_x \,. \tag{7}$$

For most initial data, the non-convexity of f causes the conserved total mass of the v_i in (5) to quickly aggregate to $K << N$ of the v_i, forming *spikes* that stay in place while changing size. Gradually some spikes disappear as the remaining ones grow, with the number of spikes, K, scaling like

$$K \sim \left(\frac{t}{N}\right)^{-\frac{1}{3}}. \tag{8}$$

The spikes in (5) corresponds to jump discontinuities in discretizations of (7). This coarsening process is well-known in the image processing community, where the creation of the jump discontinuities is known as *staircasing* (see Figure 3).

In granular flow, this coarsening corresponds to a decreasing number of shear bands in the granular medium. In population dynamics, it represents the growth of population centers, and in image processing it coincides with a simplification of the processed image – at early stages the image stays close to the original noisy image, but in later stages fine structures (including noise) disappear, leaving only the largest features.

3.2 My contribution: Weak upper bound on the coarsening rate.

Prof. S. Esedoḡlu (U. Michigan Mathematics) and I proved a one-sided time-averaged version of (8)**. Our results also apply to a discretization of** (7) **and to a two-dimensional model for locally reinforced population aggregation.** Our proof relies on a method introduced by Kohn and Otto in [17] for proving weak upper bounds on the coarsening rates of energy driven systems. Given a system length scale L and energy E, their method requires only a dissipation inequality between $\frac{dL}{dt}$ and $\frac{dE}{dt}$ and a pointwise isoperimetric inequality relating L to E. These inequalities are combined with an ODE argument to prove a time-averaged lower bound on the energy that is conceptually equivalent to an upper bound on the coarsening rate. Although we follow the method of proof outlined in [17], our problem required new arguments to prove the necessary isoperimetric inequalities, and the discrete setting distinguishes it in a substantial way from previous applications of Kohn and Otto's method. **(Submitted for publication. Preprint available on-line: [10])**

4 Current projects and future goals.

I am currently involved in projects discussed below in sections 4.1-4.2. In addition to these new directions of research, I hope to investigate many unanswered questions in my past areas of research. I discuss these interests in Section 4.3.

4.1 Curve motion

Prof. R. Kohn and I are studying the mathematics behind a recently developed method for calculating the arrival time function u of a curve $C(s)$ moving with speed $v(s) > 0$ normal to itself. This arrival time function formally solves

$$\| \nabla u \| f = 1 \quad \text{and} \quad \nabla u \cdot \nabla f = 0 \tag{9}$$

combined with the conditions

$$u(x) = 0 \quad \text{and} \quad f(x) = v(x) \quad \text{for } x \in C,$$

where the function f gives the normal velocity of C as it passes through x. Although computations of (9) are successful and have a clear geometric meaning, the solutions have discontinuities in both ∇u and f and are not covered by current viscosity solution theory for Hamilton-Jacobi equations. We hope to develop a theory of solutions for (9) analogous to standard viscosity solution theory. We are currently investigating connections (9) shares with the infinity-Laplacian equation, the statistical physics concept of mold growth, and the motion of triple points.

4.2 Schemes for conservation laws with cut cells

Many examples of compressible and incompressible flow involve domains with complicated boundaries (e.g. air flow past a jet or space shuttle). One may compute on such domains by embedding the boundary in a Cartesian grid, leaving grid cells at the boundary that are much smaller than cells away from the boundary. These small cells make standard numerical schemes for hyperbolic PDEs impractical, since they require time steps that scale with the size of the domain's smallest grid cell. Accordingly, Berger and Leveque developed finite volume *h-box methods* with time steps that are not restricted by these small cut cells [2, 3]. I am currently working with Prof. M. Berger to develop similar methods for flux-interpolation schemes similar to ENO finite difference schemes, which are typically easier to implement in higher dimensions than finite volume methods [23]. We've recently had success with a second-order flux-interpolation scheme for the Euler equations in two dimensions. Figure 4 shows results of this method on a nonuniform grid. The scheme's CFL condition depends only on a reference cell size h, even though every third cell in each direction has a size between $h/10$ and $h/3$. Our primary goal is to apply these types of schemes to domains with embedded boundaries.

4.3 Other goals.

Each of the problems discussed in sections 1-3 leaves open questions. This is a sampling of the problems that interest me:

- **Fourth-order PDEs for image denoising.** New high-order PDEs continue to be introduced in the image processing literature, but it remains to be seen whether these methods significantly improve upon the simpler second-order methods. I am interested in analyzing discretizations of these PDEs much like discretizations of their second-order analogues have been analyzed. I hope such analysis will increase understanding of these new methods and shed light on their true merit.

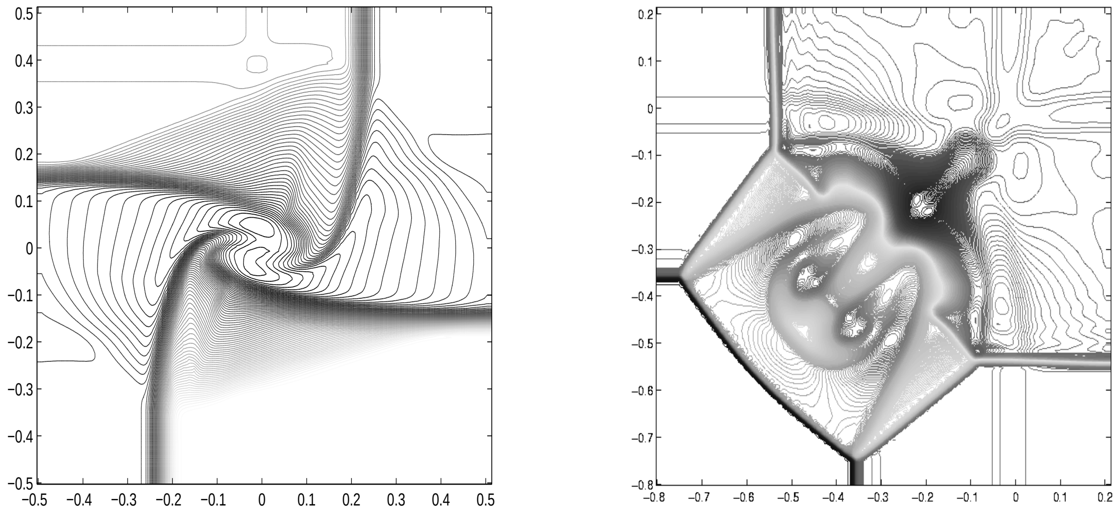

Figure 4: Each figure shows a computation of a two-dimensional Riemann problem for the Euler equations on a nonuniform grid using a flux-interpolation scheme that has a CFL condition depending only on a reference cell size h, not on the smallest cell size. The left figure shows a stage in the evolution of four jump discontinuities (one between each quadrant), and the right figure shows a stage in the evolution of four shocks. The initial conditions correspond to configurations 3 (right) and 6 (left) in [18].

- **PDEs on surfaces.** I would like to investigate a combination of the modified method for solving PDEs on surfaces (discussed in Section 2.3) with curve/surface motion. I am also interested in examining improvements of this method for surfaces with complicated geometries.
- **Coarsening of discrete ill-posed diffusions.** The work discussed in Section 3.2 concerns only an upper bound on coarsening rates. Prof. Esedoḡlu and I would like to examine the possibility of proving more about these coarsening processes; for example we may be able to prove lower bounds for specific sets of initial data. Such analysis could prove useful for those studying coarsening of other systems.

References

[1] D. Adalsteinsson and J. A. Sethian. Transport and diffusion of material quantities on propagating interfaces via level set methods. *J. Comput. Phys.*, 185(1):271–288, 2003.

[2] M. Berger and R. LeVeque. Cartesian meshes and adaptive refinement for hyperbolic partial differential equations. In *Third International Conference on Hyperbolic Problems, Vol. I, II (Uppsala, 1990)*, pages 67–73. Studentlitteratur, Lund, 1991.

[3] Marsha J. Berger, Christiane Helzel, and Randall J. Leveque. h-box methods for the approximation of hyperbolic conservation laws on irregular grids. *SIAM J. Numer. Anal.*, 41(3):893–918 (electronic), 2003.

[4] F. Bernis and A. Friedman. Higher order nonlinear degenerate parabolic equations. *J. Differential Equations*, 83(1):179–206, 1990.

[5] M. Bertalmío, L. T. Cheng, S. Osher, and G. Sapiro. Variational problems and partial differential equations on implicit surfaces. *J. Comput. Phys.*, 174(2):759–780, 2001.

[6] A. L. Bertozzi. Symmetric singularity formation in lubrication-type equations for interface motion. *SIAM J. Applied Math*, 56(3):681–714, June 1996.

[7] A. L. Bertozzi and J. B. Greer. Low-curvature image simplifiers: global regularity of smooth solutions and Laplacian limiting schemes. *Comm. Pure Appl. Math.*, 57(6):764–790, 2004.

[8] A. L. Bertozzi, J. B. Greer, S. Osher, and K. Vixie. Nonlinear regularizations of TV based PDEs for image processing. In *Nonlinear partial differential equations and related analysis*, volume 371 of *Contemp. Math.*, pages 29–40. Amer. Math. Soc., Providence, RI, 2005.

[9] S. Esedoḡlu. An analysis of the Perona-Malik scheme. *Comm. Pure Appl. Math.*, 54(12):1442–1487, 2001.

[10] S. Esedoḡlu and J. B. Greer. Upper bounds on the coarsening rate of discrete, ill-posed nonlinear diffusion equations. Submitted for publication in September 2006.

[11] D. J. Eyre. An unconditionally stable one-step scheme for gradient systems. Unpublished article, June 1998.

[12] K. Glasner. A diffuse interface approach to Hele-Shaw flow. *Nonlinearity*, 16(1):49–66, 2003.

[13] J. B. Greer. An improvement of a recent Eulerian method for solving PDEs on general geometries. to appear in J. Sci. Comput.

[14] J. B. Greer and A. L. Bertozzi. H^1 solutions of a class of fourth order nonlinear equations for image processing. *Discrete Contin. Dyn. Syst.*, 10(1-2):349–366, 2004. Partial differential equations and applications.

[15] J. B. Greer and A. L. Bertozzi. Traveling wave solutions of fourth order PDEs for image processing. *SIAM J. Math. Anal.*, 36(1):38–68 (electronic), 2004.

[16] J. B. Greer, A. L. Bertozzi, and G. Sapiro. Fourth order partial differential equations on general geometries. *J. Comput. Phys.*, 216(1):216–246, 2006.

[17] R. V. Kohn and F. Otto. Upper bounds on coarsening rates. *Comm. Math. Phys.*, 229(3):375–395, 2002.

[18] A. Kurganov and E. Tadmor. Solution of two-dimensional Riemann problems for gas dynamics without Riemann problem solvers. *Numer. Methods Partial Differential Equations*, 18(5):584–608, 2002.

[19] S. Osher, A. Solé, and L. Vese. Image decomposition and restoration using total variation minimization and the H^{-1} norm. *Multiscale Model. Simul.*, 1(3):349–370 (electronic), 2003.

[20] K. J. Painter, D. Horstmann, and H. G. Othmer. Localization in lattice and continuum models of reinforced random walks. *Appl. Math. Lett.*, 16(3):375–381, 2003.

[21] P. Perona and J. Malik. Scale-space and edge detection using anisotropic diffusion. *IEEE Trans. Pattern. Anal. Machine Intell.*, 12:629–639, 1990.

[22] L. Rudin, S. Osher, and E. Fatemi. Nonlinear total variation based noise removal algorithms. *Physica D*, 60:259–268, 1992.

[23] C. W. Shu and S. Osher. Efficient implementation of essentially nonoscillatory shock-capturing schemes. *J. Comput. Phys.*, 77(2):439–471, 1988.

[24] J. Tumblin and G. Turk. LCIS: A boundary hierarchy for detail-preserving contrast reduction. In *Proceedings of the SIGGRAPH 1999 annual conference on Computer graphics, August 8-13, 1999, Los Angeles, CA USA*, pages 83–90, 1999. http://www.acm.org/pubs/citations/proceedings/graph/311535/p83-tumblin/.

[25] T. P. Witelski, D. G. Schaeffer, and M. Shearer. A discrete model for an ill-posed nonlinear parabolic PDE. *Phys. D*, 160(3-4):189–221, 2001.

[26] J. Xu and H.-K. Zhao. An Eulerian formulation for solving partial differential equations along a moving interface. *J. Sci. Comput.*, 19(1-3):573–594, 2003. Special issue in honor of the sixtieth birthday of Stanley Osher.